



OPEN ACCESS

EDITED BY

Dipendra Gautam,
University of Iceland, Iceland

REVIEWED BY

Kshitij C. Shrestha,
Tribhuvan University (Pulchowk Campus), Nepal
Polat Gülkan,
Baskent University Hospital, Türkiye

*CORRESPONDENCE

Natividad Garcia-Troncoso,
✉ nlgarcia@espol.edu.ec

RECEIVED 14 October 2025

REVISED 05 December 2025

ACCEPTED 12 December 2025

PUBLISHED 21 January 2026

CITATION

Garcia-Troncoso N, Molina-Cedeño J,
Vergara-Pin M, Zambrano-Montalvan H,
Tello-Ayala K and Bompa DV (2026) Finite
element modelling of bahareque walls under
lateral cyclic loading.
Front. Built Environ. 11:1722178.
doi: 10.3389/fbuil.2025.1722178

COPYRIGHT

© 2026 Garcia-Troncoso, Molina-Cedeño,
Vergara-Pin, Zambrano-Montalvan, Tello-Ayala
and Bompa. This is an open-access article
distributed under the terms of the [Creative
Commons Attribution License \(CC BY\)](https://creativecommons.org/licenses/by/4.0/). The use,
distribution or reproduction in other forums is
permitted, provided the original author(s) and
the copyright owner(s) are credited and that the
original publication in this journal is cited, in
accordance with accepted academic practice.
No use, distribution or reproduction is permitted
which does not comply with these terms.

Finite element modelling of bahareque walls under lateral cyclic loading

Natividad Garcia-Troncoso^{1,2*}, Juan Molina-Cedeño¹,
Miguel Vergara-Pin¹, Hilda Zambrano-Montalvan³,
Ken Tello-Ayala¹ and Dan V. Bompa⁴

¹Faculty of Engineering in Earth Sciences, ESPOL Polytechnic University, ESPOL, Guayaquil, Ecuador, ²Centro de Investigación y Desarrollo en Nanotecnología, Escuela Superior Politécnica del Litoral, ESPOL, Guayaquil, Ecuador, ³Escuela de Ingeniería Civil, Universidad Espiritu Santo (UEES), Samborondon, Ecuador, ⁴School of Sustainability, Civil and Environmental Engineering, University of Surrey, School of Engineering, University of Surrey, Guildford, United Kingdom

This study presents a numerical representation of the cyclic behavior and energy dissipation characteristics of cemented bahareque walls using the non-linear modeling procedures. A numerical model was calibrated through experimental tests to fit the nonlinear response, including the stiffness degradation and hysteretic behavior of bahareque walls subjected to reversed cyclic loading. An additional sensitivity analysis was carried out to evaluate the influence of aspect ratio, fastener spacing, frame cross-section, mortar panel thickness, and vertical load on the structural response of the cemented bahareque walls. Results indicate that the calibrated model successfully replicates the energy dissipation capacity of the experimental walls with a relative energy error of 4.84%, despite some localized discrepancies in force predictions. The sensitivity analysis indicated significant variation in hysteretic response associated with fastener spacing, stiffness degradation parameters, and pinching effects. This study also shows that variations in parameters as fastener spacing can affect the model's lateral loading capacity by up to 23.40%. These results underscore the influence of key modeling parameters on wall structural behavior. The findings demonstrate the suitability of the calibrated numerical model for predicting global seismic demands and highlight critical parameters that influence the cyclic performance and resilience of bahareque walls for affordable housing.

KEYWORDS

bahareque wall, energy dissipation, hysteretic model, OpenSEES, parameter assessment

1 Introduction

1.1 Background

The increasing of global demand for affordable housing, particularly in seismic regions, poses significant challenges (Puri et al., 2017). Conventional construction materials are becoming scarce and environmentally costly (Yang and Wang, 2020). Therefore, sustainable construction technologies that meet structural requirements are urgently needed. In this context, vernacular building systems such as bahareque systems, incorporating natural materials, appear as a feasible solution for affordable housing in seismic areas (Kaminski et al., 2023; Shan et al., 2023).

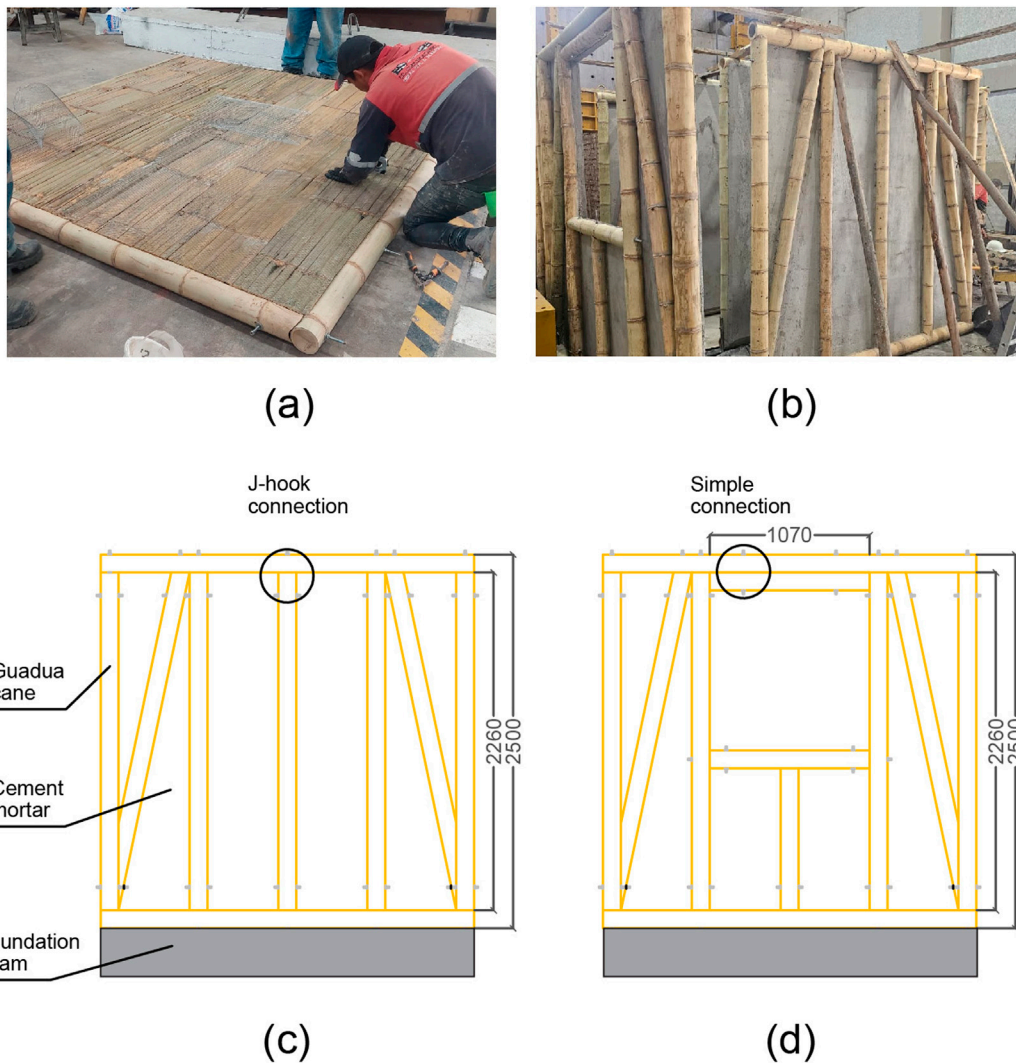


FIGURE 1
Cemented bahareque wall: (a) Guadua mat and steel mesh (b) mortar layer (c) Layout without opening (d) Layout with opening.

Cemented bahareque is a traditional structural system that adopts timber or bamboo elements with a matrix of mat or guadua strips, finished with an external plaster of cement mortar or mud that provides the wall's shear resistance (Kaminski et al., 2023). In this construction method, the bamboo or timber frame acts as the primary skeleton, while the intermediate mat, typically formed by guadua strips, serves as the base for the cementitious layers. Commonly, galvanized wire meshes are used to bond the cement mortar to the guadua intermediate mat, serving as well as a crack resisting mechanism (Mite-Anastacio et al., 2022). Compared to traditional timber frames, which often include natural stones and soil infill (Vieux-Champagne et al., 2014), cement mortar layer plastering results in practical solutions against environmental variations. This combination of materials and layers defines the mechanical behavior of cemented bahareque walls and provides the basis for the numerical modeling presented in the following section. A common layout arrangement of cemented bahareque wall is depicted in Figure 1, which is connected to a reinforced concrete

foundation and bolted to other guadua sections. Although bolted joints are the principal framing connection, other detailing mechanism exist for improved structural performance.

The main objective of a shear wall is to ensure sufficient structural stability to lateral loads such as wind and seismic loads (Resmi and Yamini Roja, 2016). A number of studies evaluated the suitability of bamboo as a main material to provide in-plane lateral stiffness, load capacity and ductility in bahareque frames (Hutubessy et al., 2014). Investigations were also carried out to evaluate the out-of-plane response (Abdul-Qadir and Saeed, 2020; González Beltrán, 2023). Guadua cane was also used in lintels (Blondet et al., 2006), slabs (Mali and Datta, 2018) and wall panels (Puri et al., 2017). Regardless of the bamboo properties, bamboo structures are controlled primarily by steel connections, since they control global failure of the system under lateral loading (Luna and Takeuchi, 2012). The influence of sheathing to framing connections were reported in many studies (Arbelaez and Correal, 2012; Di Gangi et al., 2020), as well as investigations on

frame-to-frame joints (Sharma et al., 2011), studs to loading beam, and foundation connections (González and Gutiérrez, 2005; Sharma et al., 2011).

1.2 Literature review on timber-bamboo structures

One crucial aspect overlooked in previous studies is the effect of vertical loads on shear walls performance. Experimental tests on light-frame timber walls indicated that incorporating vertical loading during testing is essential to prevent early uplift failures and accurately predict real-world behavior (Kaminski et al., 2023). In bahareque walls, the vertical loads are mainly carried by the upright bamboo frame members, since the infill and mortar layers exhibit much smaller stiffness, however, applying the vertical load in the test is still necessary to ensure realistic contact conditions, compression at the base, and appropriate load transfer between the frame and the mortar layer. Vertical loads not only enhance the wall's lateral resistance and uplift performance but ensure realistic load transfer between bamboo frames and the cement mortar (Parris et al., 2021; Poletti et al., 2016). In Romanian Traditional Framed Masonry (TFM) wall tests, uplift was observed in cyclic loading scenarios, with substantial vertical displacement in the base connections, which had impact on the lateral strength of the frames (Parris et al., 2021).

The behavior of timber and bamboo-based structures is well represented in numerical models in the literature, where the overall non-linear wall response is derived from load-deformation measurements of the connections. (Casagrande et al., 2016; Patton-Mallory et al., 1984; Zhao and Qiu, 2023). Although finite element approaches in bahareque are not yet available in the literature, timber frames and bamboo-based products, as Cross-Laminated Bamboo (CLB) sections, adopted modelling approaches that could be suitable for the work in this paper (Echeverry et al., 2017; Lu et al., 2022; Wang et al., 2019). In modelling of joints, response is typically characterized by an initial slip, rigid rotation, progressive stiffness degradation, and ultimate ductile failure modes (Hao et al., 2023; Quinn et al., 2016).

Developing a constitutive model for load-carrying shear systems is best accomplished through Finite Element Modeling (FEM). Sheathing panels and frame members are frequently represented using plane-stress and beam-type elements, respectively, presuming elastic-brittle behavior in tension and elastic behavior in compression (Gattesco and Boem, 2016). Moreover, connections are modeled through non-linear springs regarding sheathing to framing and framing to base connections (Lukic et al., 2018). For instance, Shear-Axial interaction on FEM is determined by hysteretic materials due to the capability of demonstrating the hysteretic behavior of bamboo beam-column joint, allowing for capturing the pinching effects and degradation behavior (Zhao and Qiu, 2023).

Despite the advancements in numerical modeling and experimental tests, several gaps remain in the literature regarding cemented bahareque walls. There is a notable lack of robust constitutive models that can capture the multi-scale behavior of bamboo (Sharma et al., 2015). Furthermore, a detailed representation of progressive damage in composite systems is still

underexplored (Ogrizovic et al., 2022). Moreover, integrating connection behavior with the global system response remains a challenge, as highlighted by studies focusing on the modeling of joint connections (Hu et al., 2007). Lastly, validating numerical models against full-scale seismic performance data is essential to ensure their reliability in real-world applications (Cao et al., 2022).

This paper examines the numerical response of cemented bahareque walls using the OpenSees framework, by incorporating non-linear material and elements by implementing hysteretic behavior. By comparing experimental test data, it is assessed with the energy dissipation in sheathing-to-framing connections as well as quantified the ductility and equivalent viscous damping of the wall system under seismic loads, resulting in practical findings for their design and analysis. In addition, a sensitivity analysis with respect to structural arrangement and resulting cost is carried out, considering typical geometries for affordable housing configurations. The research contributes to the broader goal of establishing reliable design methodologies for sustainable building systems.

2 Numerical modeling

In this section, cemented bahareque walls are modelled in Open System for Earthquake Engineering Simulation (OpenSees) adopting non-linear procedures to assess their behaviour and failure modes in response to cyclic loading (McKenna et al., 2025). Relevant considerations in the software workflow are also discussed to ensure realistic simulation of the specimens. OpenSees is an object-oriented framework that uses finite element analysis for earthquake engineering simulations. It was selected because it is open-source and facilitates large-scale analyses (McKenna, 2011). Moreover, its recent widespread use in seismic assessments of various structural systems has also been reported in the literature (Cristancho et al., 2025; Guan et al., 2024; Shabani and Kioumars, 2022; X. Yan et al., 2024).

The models are based on experimental tests of Cemented Bahareque Walls under reversed cyclic loading at Housing Research Center (CIV) in Quito, Ecuador, where a total of 8 specimens were tested with a uniform vertical load at the top of the wall, and a reversed cyclic loading protocol in displacement control according to ASTM 2126 standard, that would then be used to obtain the hysteresis of each wall configuration. To make the CUREE Basic Loading Protocol, it was first estimated the yield displacement through a monotonic test, and afterwards the protocol was built from 5% to 100% of the yield displacement, followed by incremental displacements considering an α factor.

As depicted in Figure 1, the 2,500 × 2,500 mm cemented bahareque walls were made in two types of configurations: Type BW1 referred to a bahareque wall without an opening made of bamboo elements at the frame, J-hook connections, staples, and cement mortar overlay; Type BW2 referred to a bahareque wall with an opening of 1,070 × 1,070 mm with the only difference of having a double cane section at the lintel of the opening. The testing arrangement consisted on a foundation anchored to the reaction slab, the bahareque wall, a loading pine wood profile for the vertical load, horizontal and vertical actuators, lateral bracing, and the instrumentation for displacement measurement through four

TABLE 1 Bahareque Wall experimental properties.

Parameters	Value
Geometric properties	
Wall length	2,500 mm
Wall height	2,500 mm
Bamboo diameter	120 mm
Guadua mat thickness	10 mm
Mortar layer thickness	25 mm
Materials	
Wall frames	Guadua angustifolia kunth
Mat	Guadua angustifolia kunth
Wire mesh	Steel
Connections	Steel
Coating layer	Mortar
Experimental setups	
Tests	10
Reinforcement	Steel rods and mortar infill
Vertical loading	14.71 kN
Loading tests	Monotonic and cyclic
Displacement protocol	CUREE basic loading protocol

Linear Variable Differential Transducers (LVDTs), one for the vertical displacement, and three for horizontal displacements at top, middle, and lower parts of the wall.

Those specimens were built according to the specifications described in Table 1, where certain walls were tested additionally on reinforced condition by anchoring the wall with steel threaded rods, as the main failure was related to the early detachment of the mortar layer due to connection failure under large displacements that reached about 200 mm, with a mean peak force of 10 kN. Some observed damage patterns as bent rods and mortar cracks, indicated an adequate energy-dissipation capacity in the sheathing-to-frame and internal release connections, as for other observations in the hysteresis behavior indicated that walls without reinforcement or with openings lacked a pronounced plateau, suggesting a quick degradation after their peak force on the loading protocol. Based on these results and configurations, it is defined that the numerical model must allow the interaction of frame and shell elements under similar properties, materials, displacements and forces of the experimental tests.

2.1 Modeling strategy and loading

The workflow used to develop the model consists of eight stages, illustrated in Figure 2, with the final stages including a brief description of their associated commands iterating the most influencing parameters. The wall's reliable performance under lateral loads through the effective interaction of all its

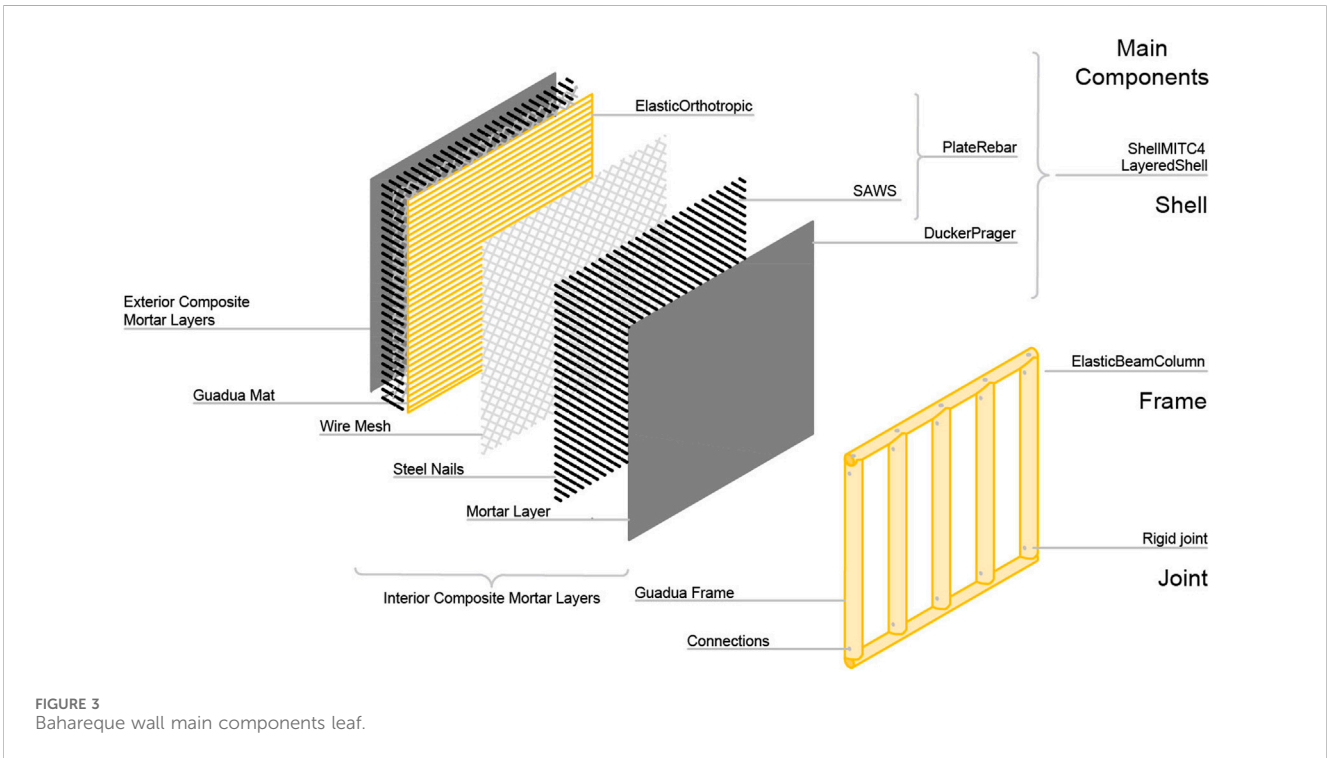
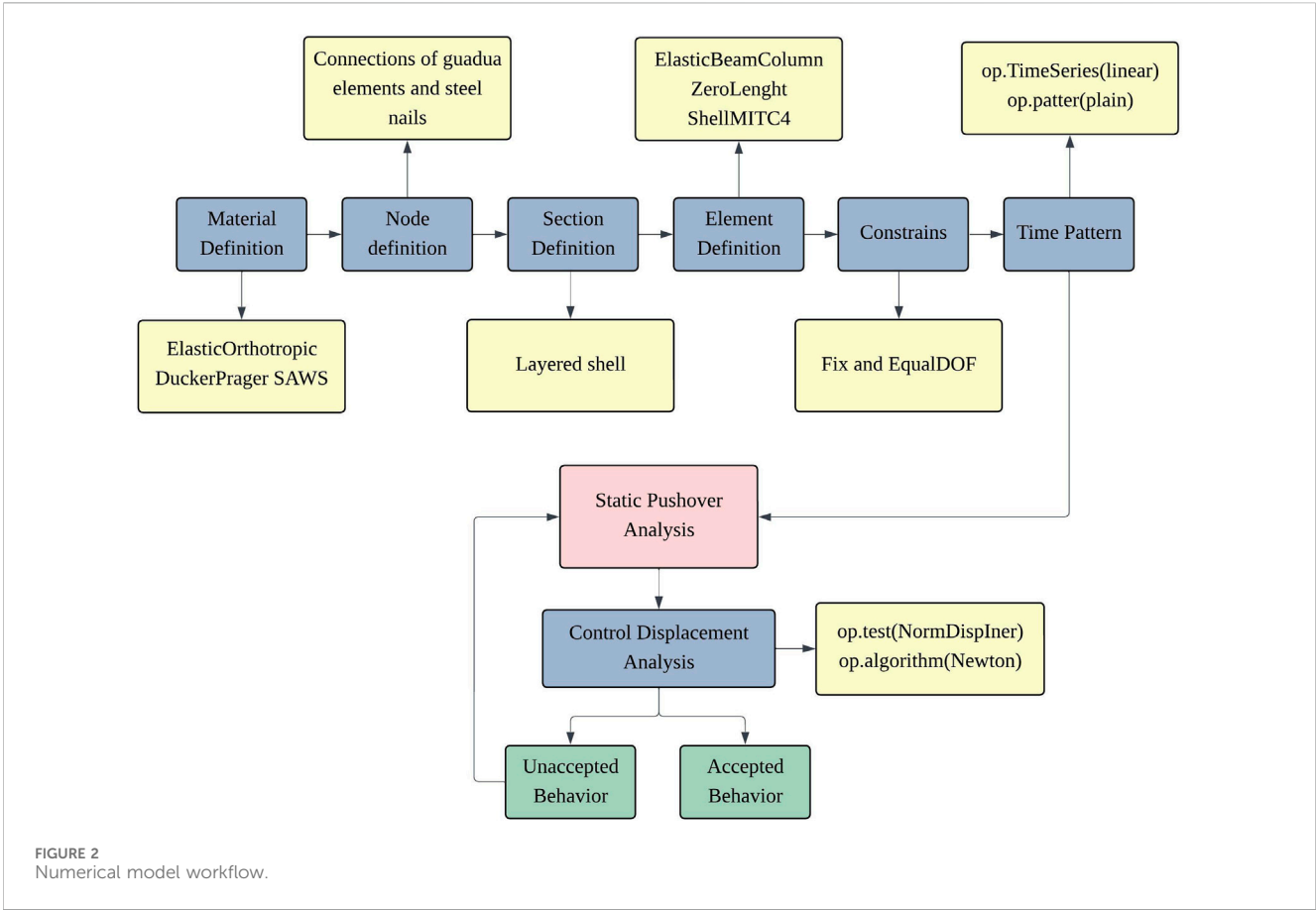
components. To achieve this, an advanced nodal configuration was employed to consider the sheathing-to-frame connections, as well as frame-to-frame connections.

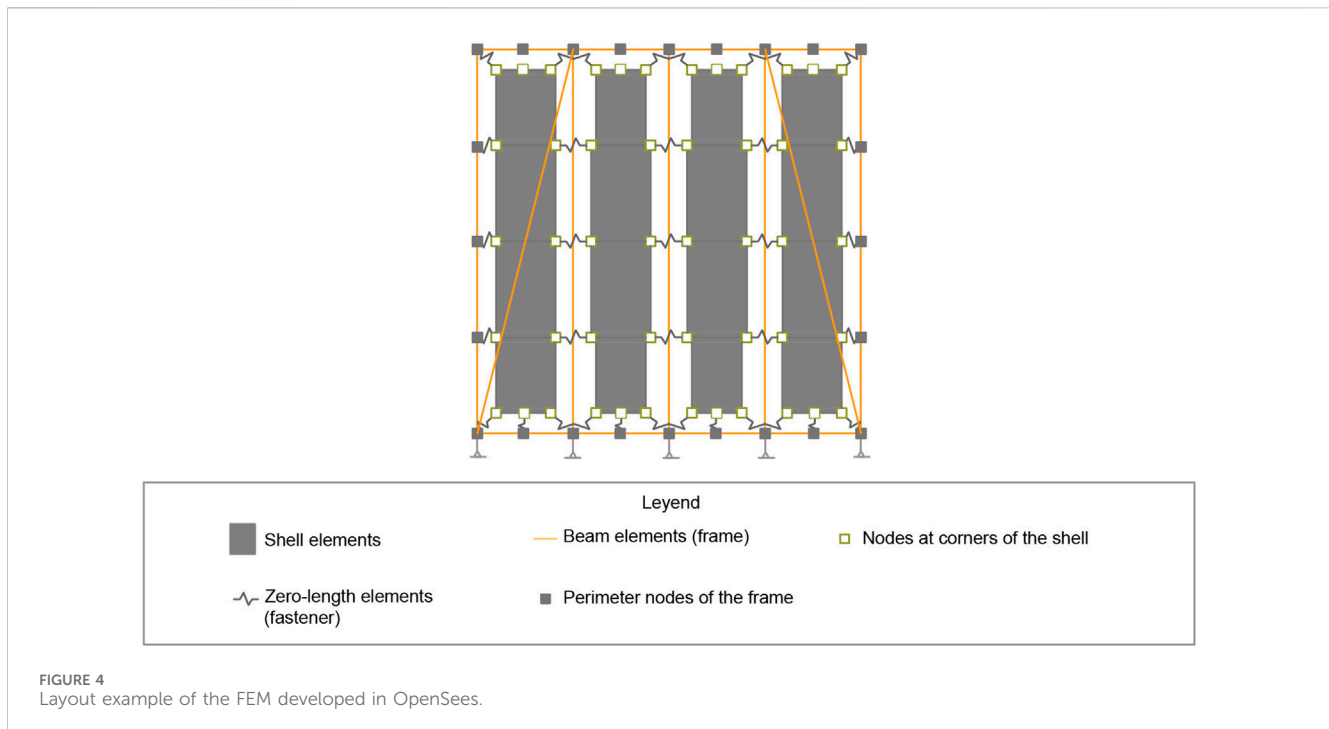
To achieve this, an advanced nodal configuration was employed to consider the sheathing to frame connections, as well as frame to frame connections. The modelling strategy adopts the following sequence: (1) define the uniaxial materials such as Steel01 which is a bilinear steel model with kinematic hardening, DuckerPrager defined as a pressure dependent plasticity model, and SAWS as a nonlinear hysteretic spring model in OpenSees that represents the cyclic stiffness degradation, pinching, and strength loss typically observed in shear-type connections and joint assemblies.; (2) define the nodes to represent frame-frame, panel-frame, and panel-panel connections; (3) define the sections as a superposition of multiple layers by using LayeredShell section through ShellMITC4 element; (4) define the elements such as ElasticBeamColumn and ZeroLength to represent the assembled frame; (5) assign constraints and EqualDOF to nodes regarding the foundation connection and the overturning restraints according to experimental tests conditions, as it enforces identical degrees of freedom between nodes; (6) specify the time pattern of load application using the Linear TimeSeries and Plain Pattern commands; (7) review of numerical effectiveness based on the scheme of hysteresis curve; and (8) analysis of control displacement parameters as tolerance, iterations steps and displacement step size using the NormDispIncr Test and Newton algorithm.

The convergence test used in the analysis was the NormDispIncr criteria, with a displacement-norm tolerance of 1×10^{-6} and a maximum of 100 iterations per step. These values ensured convergence under significant nonlinear deformation and crack opening. During cyclic loading, the solver employed the Newton algorithm with the initial tangent, and switched to ModifiedNewton or NewtonWithLineSearch whenever convergence difficulties appeared, following the fallback logic embedded in the analysis loop. Solver settings included the BandGeneral system for equation storage and solution, RCM numbering for matrix bandwidth reduction, and the Plain constraints handler. The integrator was set as LoadControl, with incremental displacement steps automatically adjusted in case of non-convergence, following the limits between the minimum and maximum step sizes defined in the analysis script. Additionally, in case of convergence problems, the step is marked as unaccepted behavior and is reduced until the solver reaches equilibrium.

2.2 Rationale of design selection

As it is intended to achieve a reliable model, the global FEM model is built and validated through experimental data previously obtained from seven $2.5 \text{ m} \times 2.5 \text{ m}$ cemented bahareque wall tests and one guadua wall frame (Zambrano et al., 2025), from which only the force and displacement datasets of three walls with no openings were used for model validation. These specimens varied in terms of characteristics: with an opening, excluding it and excluding both opening and coating, however, at the present study it will be considered only the full wall design through a representative hysteresis curve based on the experimental tests of that type of specimen. The





wall configuration consists of horizontal, vertical, and diagonal bamboo elements assembled by both simple and J-hook mortar embedded connections with steel threaded rods. This connection was opted since it was shown to increase bearing capacity on steel-concrete composite shear walls (Farnam and Khorshidi, 2023; Yan et al., 2015). Furthermore, the front side of the wall is composed of a multi-layer section. This composite section consisted of a dual exterior mortar layer followed by dual wire mesh and an interior guadua mat, held by 750 steel nails distributed throughout all the section spaced from 30 to 50 mm, which provides stiffness to lateral loads. To ensure a good connection between frame and composite mortar, additional steel nails were used around the perimeter of the frame. A visual representation of the wall design is presented in Figure 3 and the corresponding computational scheme in Figure 4.

To replicate testing conditions, the FE model incorporates the cyclic loading pattern used in the experiments, defined by ASTM 2126 (ASTM International, 2019). This pattern includes displacement increments of 5, 7.5, 10, 20, 30, 40, 70, and 100% of the yield displacement, following the CUREE Basic Loading Protocol (Method C) by increasing displacement levels (ASTM International, 2019). The yield displacement was determined from a monotonic test performed on a bamboo frame representing the skeleton of the infilled bahareque wall. As for the vertical load, it was stated to set less than 10% of the maximum axial load capacity of the vertical guadua frames according to the NEC-SE-GUADUA regulation (MIDUVI, 2015). This vertical load which is 14.71 kN is distributed in nodal forces at the top nodes of the wall. Although the axial load capacity of the guadua uprights is considered for defining the load magnitude, the vertical stress is mainly taken by the mortar, which provides the primary compressive reaction during testing.

The selection criteria for these parameters and additional (e.g., dimensions, loads, connection type) were based on the idealization of the structure under realistic conditions in the basis of typical housing representation. The dimensions and resulting loads reported by a study by Mite et al. (Mite-Anastacio et al., 2022), examined the actual demands of local communities and the recommendations of current regulations such as the NEC (2015). In addition, loads from two-story dwellings were considered such as resulted from roof, first floor walls, mezzanine diaphragm, ground floor walls and foundation. Secondly, calculations were carried out based on guidelines and resulted in a value of 14.7 kN for the vertical load, which was applied in the experimental program.

2.3 Constitutive modelling

2.3.1 Material constitutive for guadua mat, mortar and steel nails

To capture the nonlinear behavior of the reinforcement provided jointly by the guadua mat, that was based on the materials tests made by Zambrano et al. (2025) and by considering the NEC-SE. GUADUA standard for the guadua properties in Quito, Ecuador, the ElasticOrthotropic material is used for the layer definition Table 2. On the other hand, the Ducker-Prager material accounts for the specific nature of mortar materials tested as mortar cubes, allowing the simulation of both elastic and plastic response Table 3. By employing the conical yield surface in the p - q space, the Drucker-Prager model captures the initiation and evolution of plastic flow as well as post-failure strength degradation under triaxial stress paths (Adheem et al., 2022). For the nails, the SAWS uniaxial material was adopted, which is a Single Degree of Freedom (SDOF) hysteretic model developed by CUREE capable of predicting the dynamic characteristics of light-frame

TABLE 2 Parameters for guadua mat.

Parameters	Description	Definition
matTag	Unique identifier for the material instance	3
Ex	Elastic moduli in three mutually perpendicular directions (x, y, and z)	3.84 GPa
Ey, Ez		1.50 GPa
Vxy, vyz, vzx	Poisson's ratios	0.25
Gxy, Gyz, Gzx	Shear moduli	1.20 GPa

TABLE 3 Parameters for mortar layer.

Parameters	Description	Definition
matTag	Unique identifier for the material instance	5
E	Yield stress of the material	1.40 GPa
nu	Poisson ratio	0.20
K	Bulk modulus	2.52 GPa
G	Shear modulus	3.36 GPa
sigmaY	Yield stress	14.9 MPa
rho	Frictional strength parameter	0.05
rhoBar	Controls evolution of plastic volume change, $0 \leq \rho_{\text{Bar}} \leq \rho$	0.02
Kinf	Nonlinear isotropic strain hardening parameter, $K_{\text{inf}} \geq 0$	0.00
Ko	Nonlinear isotropic strain hardening parameter, $K_o \geq 0$	0.00
delta1	Nonlinear isotropic strain hardening parameter, $\delta_{\text{delta1}} \geq 0$	0.08
delta2	Tension softening parameter, $\delta_{\text{delta2}} \geq 0$	0.08
H	Linear strain hardening parameter, $H \geq 0$	-0.06*E
theta	Controls relative proportions of isotropic and kinematic hardening, $0 \leq \theta \leq 1$	0.30
density	Mass density of the material	20 kN/m ³

wood buildings (Aranha et al., 2016). Due to having influence in both vertical and horizontal reaction, the zero length elements are set with direction 1 and 2, while the directions 3, 4, 5 are set as equalDOF for the connected nodes.

2.3.2 Conceptualization of guadua frame

ElasticBeamColumn was defined as the numerical representation of guadua members. First, this allows to input many parameters that provide sufficient information about mechanical and geometric properties of guadua cane. It allows greater lateral displacements and flexibility (Shamim and Rogers, 2013) which is essential when representing hysteretic performance of bahareque wall, as the main stress localizations are at the joints. Also, as a conservative decision, the guadua frame section is set with 110 mm to provide a lower bound response due to inhere variability in diameters along the frames.

2.3.3 Wall elements

The composite nature of the mortar requires a description of multiple layers to represent the transversal section of guadua

mat and mortar layer. By doing so, this multidimensional approach required could be achieved by integrating Layered Section. In fact, it has been previously reported that hysteretic behavior simulation under cyclic loading provided by this material is desirable due to the accurate action of stiffness loading/reloading (Yu et al., 2023) as their validation study demonstrated that LayeredShell-based models can capture degradation, pinching, and stiffness patterns consistent with experimental observations in reinforced concrete shear walls. This aligns with the present study because the bahareque wall also exhibits stiffness deterioration under reversed cyclic loading, making the same modelling principle applicable to the mortar-guadua mat composite layers. As it is depicted in Figure 5, it is solely determined by external mortar layers and dual interior mat layers with different properties and thickness (t).

On the basis of three-dimensional compatibility, the ShellMITC4 element was chosen to model the layers of composite mortar panels. This choice was preferred over other alternatives since it can more accurately capture nonlinear

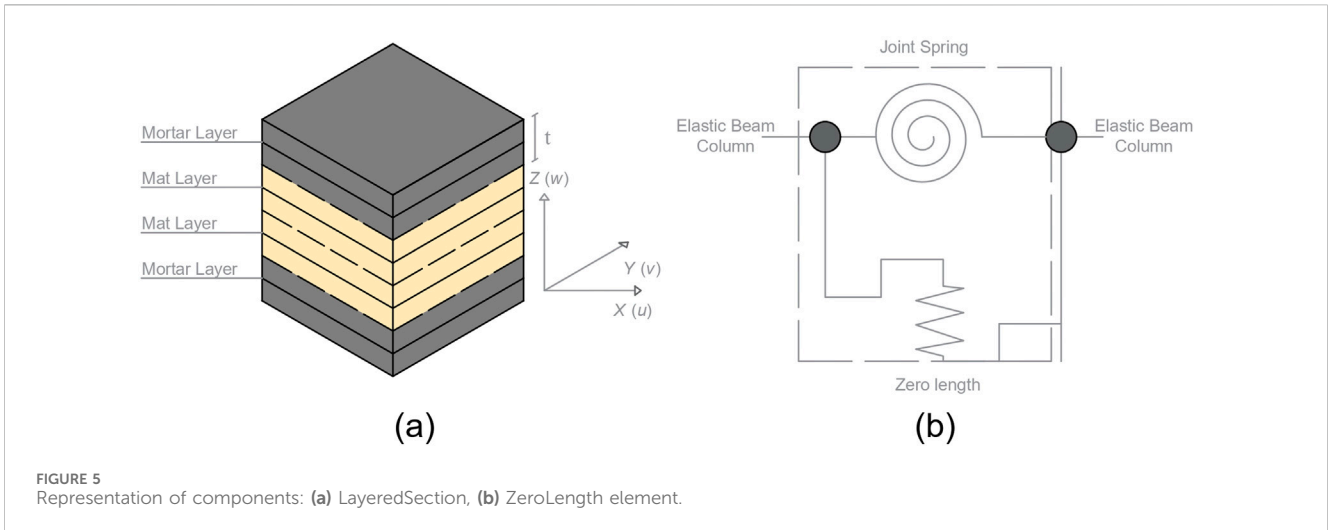


TABLE 4 Parameters for Layered Shell section.

Parameters	Description	Definition
secTag	Unique identifier for the shell section	20
numLayers	Number of layers in the shell section	3
matTag1	Identifier for the material assigned to the first layer	4
thickness1	Thickness of the first layer	0.025 m
matTag2	Identifier for the material assigned to the second layer	6
thickness2	Thickness of the second layer	0.010 m
matTag3	Identifier for the material assigned to the third layer	4
thickness3	Thickness of the third layer	0.025 m

coupling between in-plane shear, flexural, and out-of-plane responses (Yang et al., 2023). An application of ShellMITC4 with parameters in Table 4 has been used to reflect reinforced concrete walls response at lateral loads (X. Lu et al., 2015). Besides, employing a higher number of degrees of freedom in Layered Shell, issues as elevated rigidity in a bidimensional model are avoided. A further rationale for choosing this formulation is that the constitutive models used have been previously validated in similar layered-wall simulations and allow consistent interaction between mortar layers, bamboo strips, and the connections. It is highly important to ensure that modeled materials are compatible at meeting boundary conditions such as the fully fixed base used to replicate the experimental clamping of the wall specimen, the lateral restraint that prevents rigid-body overturning, and the displacement-controlled loading applied at the top node.

2.4 Joint and frame model calibration

As conservative results are expected, hysteretic joint behavior requires correct calibration. For this purpose, it was necessary to use values obtained from cyclic loading tests on 5 mm diameter screws

connected to ply CLT blocks (Dong et al., 2021), while modified according to experimentally reversed cyclic tests conducted on bahareque walls. The calibration process consisted of iteratively adjusting the SAWS parameters so that the numerical hysteresis curves matched the experimental force-displacement response obtained from the reversed cyclic tests of full-scale bahareque walls without openings. The comparison focused on initial stiffness, pinching intensity, unloading stiffness, and maximum displacement capacity, ensuring that each SAWS parameter reproduced the same features observed in the laboratory tests. The main parameters of SAWS were defined and are presented in Table 5. To a better understanding of the material and its calibration a scheme is presented in Figure 6 which depicts the construction of a SAWS curve.

All nodes are tagged according to the elements they are connected to, in this case it is separated between the frame and the sheathing grid Figure 7. The position of all those nodes is based on the geometric parameters such as height, width, fastener spacing, section sizes, shell layer, or loading. In the case of the elements, they are tagged by the number of the horizontal frame, the number of vertical frame, the left side shell elements, the right side shell elements, left side zero-length elements, and the right side zero-length elements.

TABLE 5 Parameters for SAWS model.

Parameters	Description	Definition
matTag	Integer tag identifying material	888
F0	Intercept strength of the shear wall spring element for the asymptotic line to the envelope curve $F0 > FI > 0$	1.00 kN
FI	Intercept strength of the spring element for the pinching branch of the hysteretic curve. ($FI > 0$)	0.1 kN
DU	Spring element displacement at ultimate load. ($DU > 0$)	0.002 m
S0	Initial stiffness of the shear wall spring element ($S0 > 0$)	500 kN/m
R1	Stiffness ratio of the asymptotic line to the spring element envelope curve. The slope of this line is $R1 S0$. ($0 < R1 < 1.0$)	0.10
R2	Stiffness ratio of the descending branch of the spring element envelope curve. The slope of this line is $R2 S0$. ($R2 < 0$)	-0.025
R3	Stiffness ratio of the unloading branch off the spring element envelope curve. The slope of this line is $R3 S0$. ($R3 > 0$)	0.75
R4	Stiffness ratio of the pinching branch for the spring element. The slope of this line is $R4 S0$. ($R4 > 0$)	0.03
Alpha	Stiffness degradation parameter for the shear wall spring element. ($Alpha > 0$)	0.08
Beta	Stiffness degradation parameter for the spring element. ($BETA > 0$)	1.05

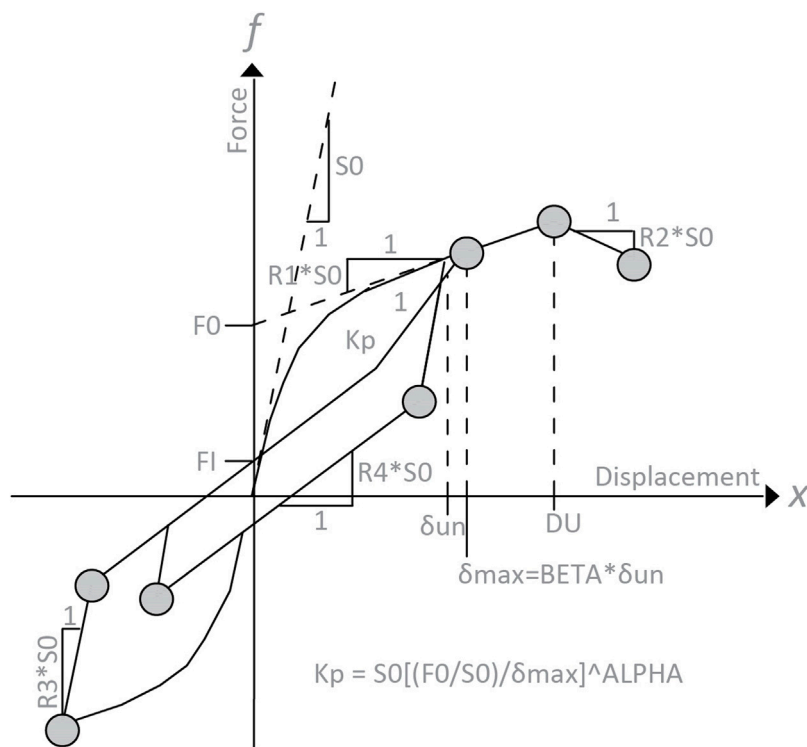


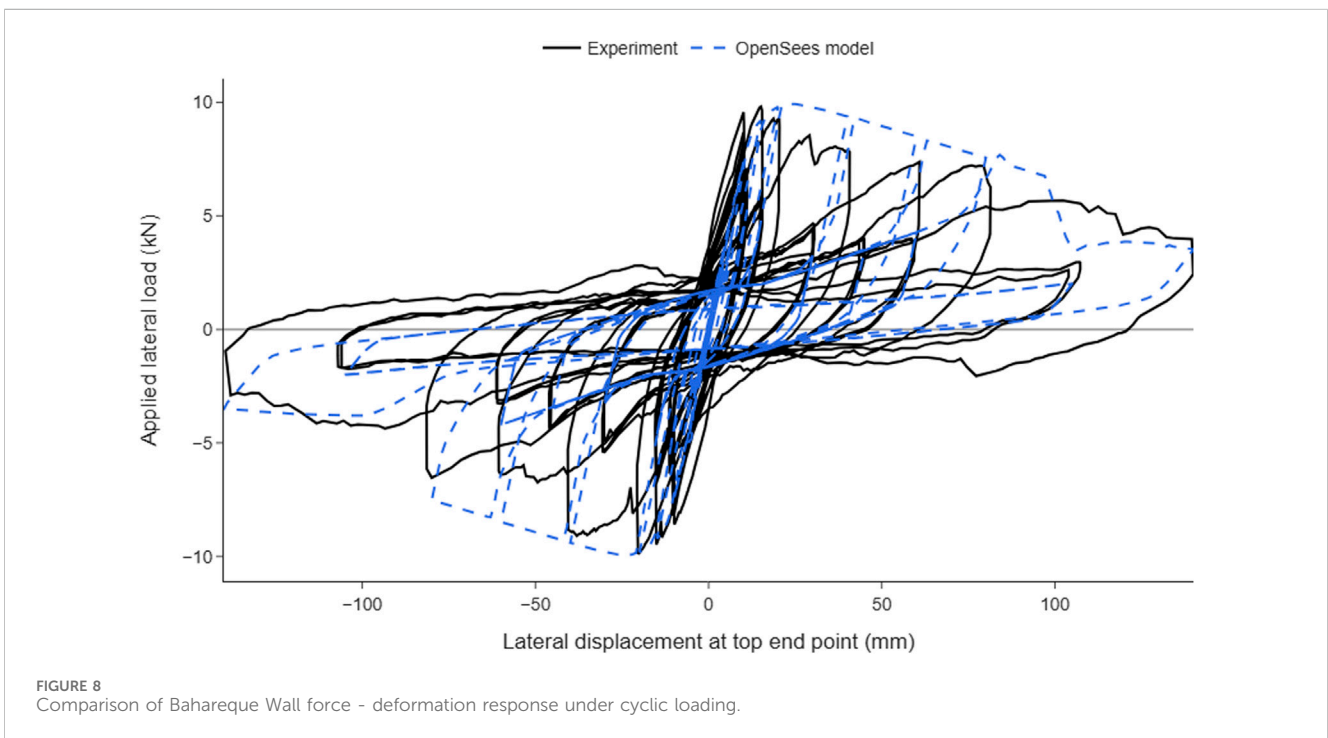
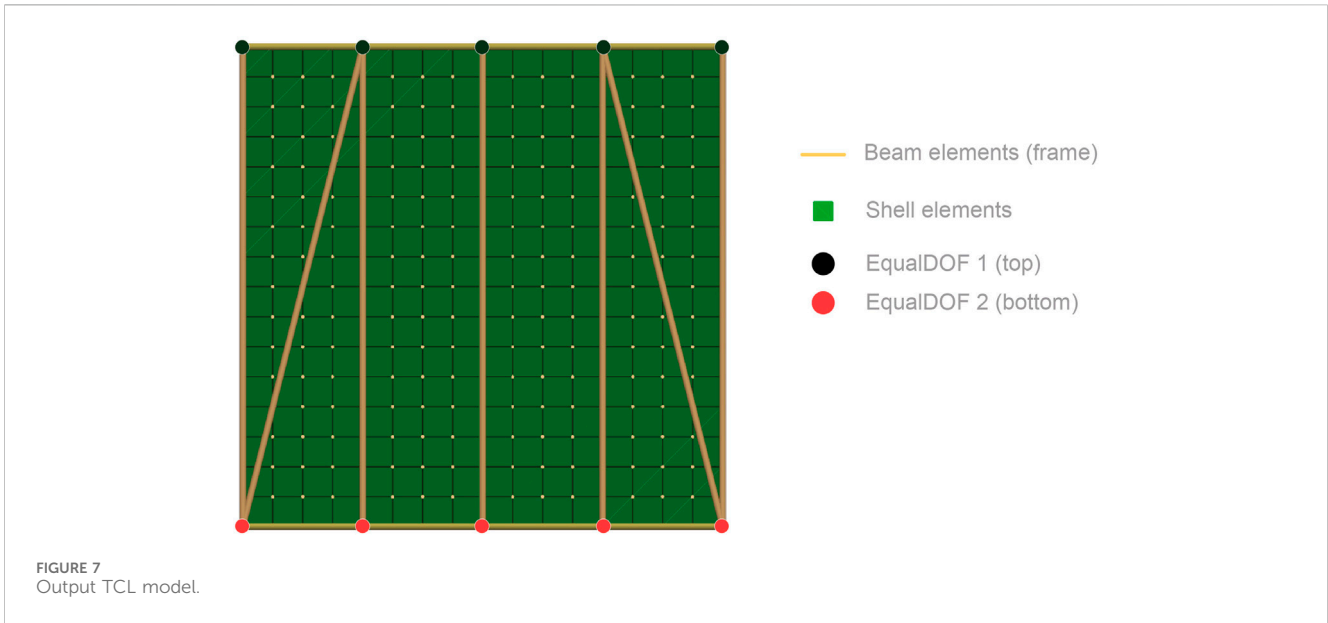
FIGURE 6 SAWS hysteresis model envelope curve.

Furthermore, it is necessary to emphasize the simplifications that have been made in the numerical model, namely the reduction of nodes for the shell elements and thus the reduction of vertical and horizontal fasteners. In addition, in order to provide greater stability, the joints between the guadua canes were defined as numerically rigid, being defined by means of equalDOF, which isolates the response to the fasteners.

3 Numerical results and optimization

3.1 Numerical validation

Once the numerical model was established, it was compared with the experimental results. This comparison is given in the Figure 8, which indicates that the non-linear behavior of the



model represents a reasonable simulation of the proposed walls. To compare the differences, it is proposed to measure the relative error for the peak force, as well as a comparison between the cumulative hysteretic energy from both curves.

The calibration process employs the modifications of the Ducker Prager and SAWS parameters in accordance with the experimental behavior of the bahareque wall. While validation involves the measurement of the cumulative dissipated energy of both experimental and numerical walls.

In Figure 9, the cumulative dissipated energy from the OpenSees model exceeds the experimental energy by 28.4 J, leaving a relative energy error of 4.84% while having a 1.3% of relative error in the positive peak force and a 0.8% of relative error in the negative peak force, which demonstrates a robust prediction capability for being below 10% in (Oh et al., 2023). This means that the model maintains higher stiffness along its displacement compared to the experimental test, mainly provided by the fasteners as it keeps more residual resistance after the ultimate displacement.

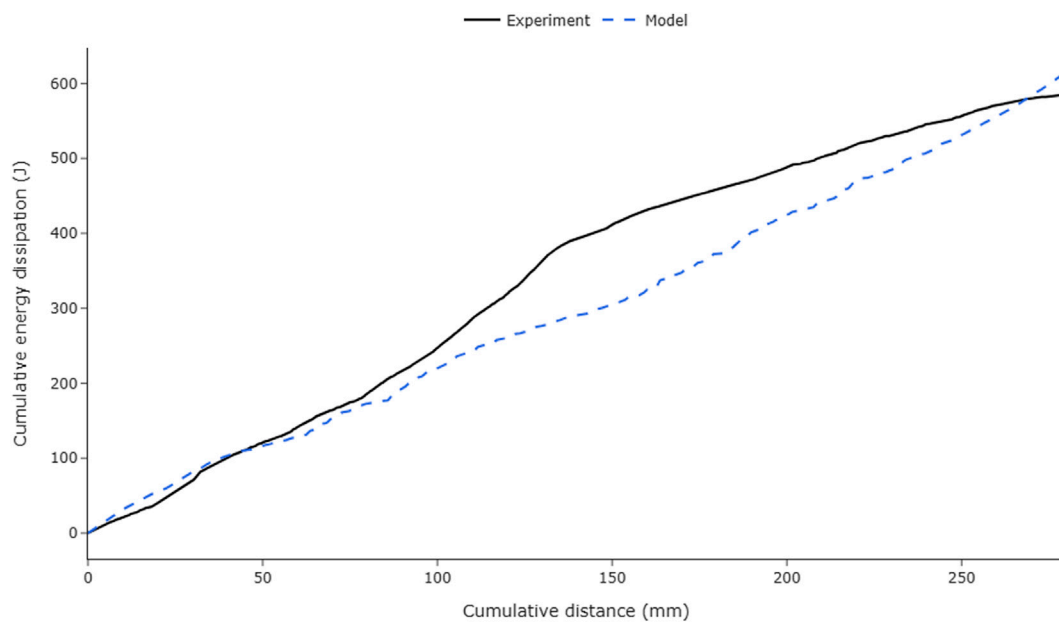


FIGURE 9
Comparison of Bahareque Wall cumulative energy dissipation.

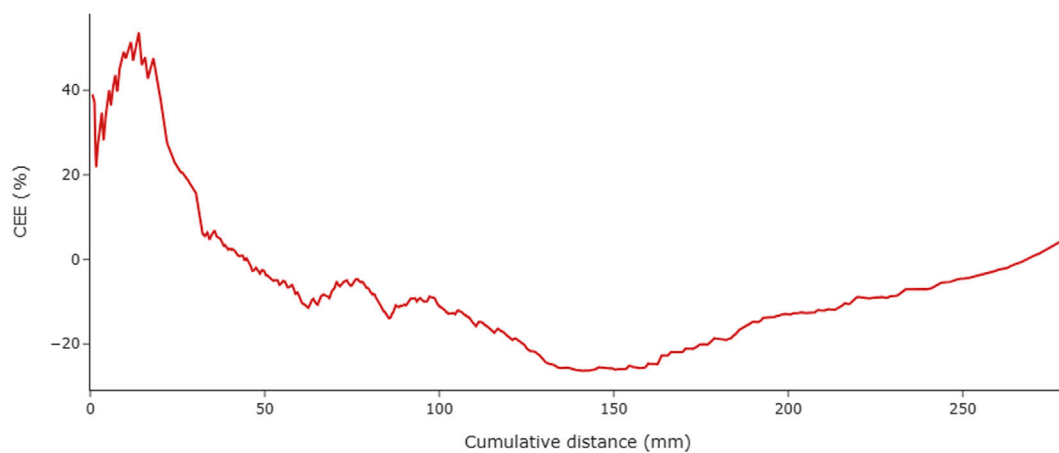


FIGURE 10
Cumulative energy error (CEE).

This highlights the need for further refinement of the model parameters in future studies. The results confirm that the finite element model effectively captures the structural dissipation behavior of elements such as fasteners under lateral loading conditions. This provides a strong foundation for conducting additional parametric studies to evaluate the hysteretic response of numerical bahareque considering materials like Pinching4 as well as other experimental tests.

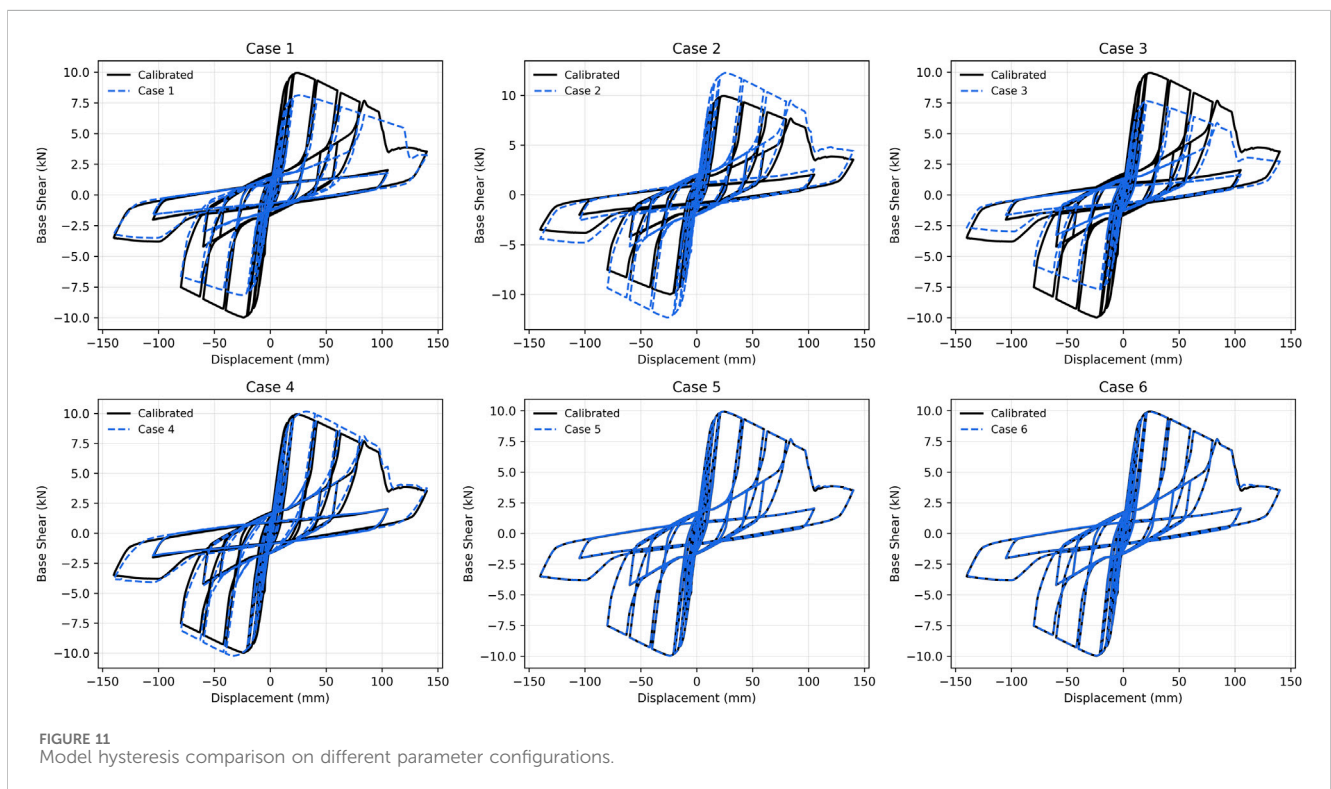
The validated numerical model is employed to investigate the energy dissipation capacity of cemented bahareque walls through a parametric analysis. This analysis examines the influence of wall geometry, connection characteristics, and material properties on the structural performance of the walls. The study begins with a

reference configuration based on a bahareque wall without openings, incorporates the same dimensions and material properties, and simplifies connections between frame and shell elements. Horizontal reversed cyclic loading is applied under displacement-controlled conditions to simulate the behavior of the walls under seismic action.

Figure 10 presents the Cumulative Energy Error of the OpenSees model, showing that despite the result in terms of energy response, it still has some discrepancies in the initial and middle sections that compensate for the overall results. It is important to note that CEE is a signed relative error, not the cumulative energy itself; therefore, its value may rise or fall depending on the incremental difference between the numerical and experimental energy at each cycle.

TABLE 6 Parameters assessment relative error.

Case	Maximum force (kN)	Difference (kN)	Relative error (%)
Case 1	8.16	-1.82	-18.26
Case 2	12.31	2.33	23.40
Case 3	7.70	-2.28	-22.87
Case 4	10.24	0.26	2.60
Case 5	9.98	0.01	0.05
Case 6	9.95	-0.02	-0.25



Therefore, the model is suitable for assessing ductility demands and global performance studies, but for applications requiring more accurate responses it is recommended to refining the degradation and pinching properties of the model.

3.2 Sensitivity analysis

The principal focus of the sensitivity analysis includes the geometric parameters of the wall, such as aspect ratio, fastener spacing, frame cross section, mortar thickness, and vertical load. Given the accuracy of the model, and the interest in obtaining the best configuration for the construction and future testing of a scale model house, it is necessary to know the influence of these parameters on the response of the bahareque wall.

The sensitivity analysis explores the influence of various parameters on the overall structural response Table 6, separated into 6 cases as these variables were selected as they directly influence stiffness, energy dissipation, and failure mechanisms in bahareque walls, following a single variable approach similar to previous parametric studies on RC shear walls (Yang et al., 2023).

- Aspect ratio $\alpha = H/L$. Varying the aspect ratio from 1.00 to 1.25 shows that a higher aspect ratio decreases strength capacity by 18.26%. This is attributed to an increased instability, as overturning becomes more prominent with higher aspect ratio.
- Effect of Fastener spacing. Varying the fastener spacing has a significant impact on wall stiffness and strength. Reducing the spacing from 156.25 mm to 125 mm increases stiffness and strength by approximately 23.40%, as the additional horizontal

TABLE 7 Unit costs of materials for bahareque construction.

Material	Unit	Unit cost (USD)
Guadua cane d11-12 cm	m	0.92
Guadua mat	m ²	2.50
Nails	kg	2.36
Threaded rod 3/8 inch	m	2.89
Steel wire mesh	m ²	2.50
Mortar 1:3 (15 mm thickness)	m ²	1.83

and vertical zero-length elements distribute loads more effectively along the frame. Conversely, increasing the spacing to 200 mm reduces stiffness and force capacity by approximately 22.87%, since the removal of zero-length elements diminishes load sharing and causes localized overstress exceeding the material strain limits. Frame cross-section size. Reducing the frame element’s cross-section size from 110 mm to 100 mm results in 2.60% increased capacity. This reflects the critical role of guadua cane size in maintaining wall stiffness and overall capacity.

- Thickness in Mortar Panel. Decreasing the mortar layer thickness over the guadua mat from 25 mm to 15 mm results in only a negligible change in capacity less than 0.1%, indicating that such small variations in mortar thickness do not produce a physically meaningful difference in the wall’s cyclic response. The initial stages of behavior remain essentially unchanged.
- Vertical Load. Incrementing vertical loads ranging from 14.71 kN to 24.52 kN slightly impacts capacity by 0.25%. Higher vertical loads contribute to better support against overturning, but excessive loads can lead to premature local failures, particularly in regions with stress concentration.

The detailed geometry of the structural elements, including the quantity of fasteners and reinforcement variation, significantly influences the behavior as seen in Figure 11. The inclusion of varying reinforcement quantities and loading conditions allows the model to simulate a broader range of structural scenarios. The change in fastener spacings or change in fastener diameter in cases 2 and 3 have shown a significant impact on the resistance of the walls, as they are the key elements in the bahareque behavior against lateral loads. Also, it changes the degradation of the model, giving a significant advantage against seismic loads. On the other hand, changes incorporate in cases 4, 5, and 6 with respect to the baseline model had lower contribution too much to the overall capacity. Despite that, it seems that it is possible to reduce both guadua section and mortar thickness without severe reductions in the bahareque capacity.

3.3 Optimized configuration

The design of cemented bahareque walls is formulated as a multi-objective optimization problem. This approach aims to balance conflicting objectives, maximizing shear capacity while minimizing total material costs. The unit costs of materials were obtained directly from certified local construction providers in Ecuador (2025). Table 7 summarizes the materials, their measurement units, and unit prices as reported by suppliers. This approach ensures that the cost analysis reflects real market conditions rather than theoretical estimates.

A solution is considered Pareto optimal when no other configuration improves one objective without compromising the other. This optimization framework provides designers and manufacturers with a range of efficient wall configurations tailored to structural and economic requirements. The design space for cemented bahareque walls includes several geometric, material, and loading parameters to optimize performance and

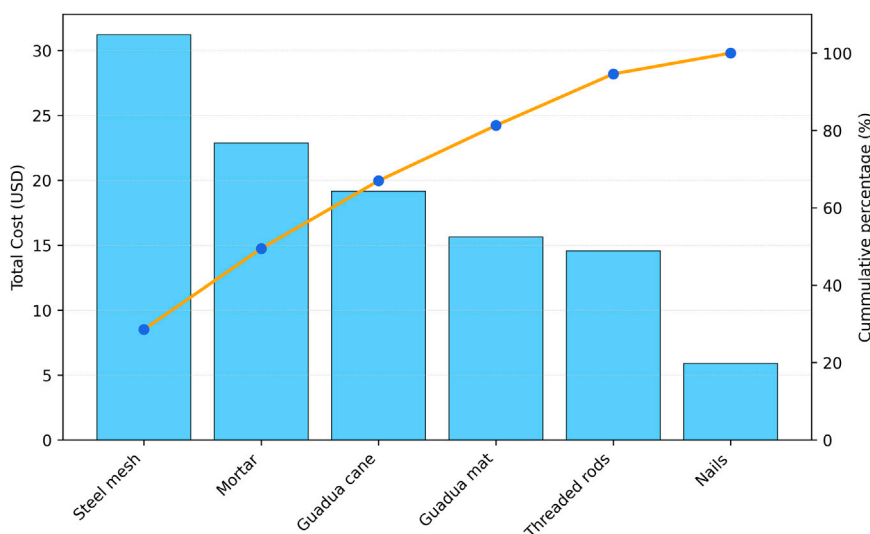


FIGURE 12 Bahareque wall pareto chart.

cost. Fastener spacing, both horizontal and vertical, is considered in three discrete values: 200 mm, 150 mm, and 125 mm. Reducing fastener spacing improves shear capacity by increasing the number of fasteners along the perimeter, which enhances load transfer efficiency while preventing early detachment of the guadua mat.

Cross-section sizes of frame elements are evaluated for external and internal vertical studs with dimensions ranging from 100 mm to 110 mm. Larger cross-section sizes enhance stiffness, particularly in walls subjected to high lateral loads, but have limited contribution on the capacity according to the simulation. Despite that result, it is highly recommended to have a larger cross-section as it is important for a higher allowable perpendicular compressive stress at the guadua-guadua joints and sheathing to frame connections.

Other parameters like mortar thickness may contribute largely to the cost optimization as well as to the reduction in CO₂ impact on the project. Regardless of the results, the use of mortar as a layer still contributes to the rigidity of the system and the out of plane stresses, as shown at experimental results where the layer was subjected to cracking at large displacements.

The optimization process evaluates the full set of wall configurations within the discrete design space, extracting non-dominated (Pareto optimal) solutions. Each configuration is analyzed using validated FEM to calculate shear capacity. As shown in Figure 12, the reduction in the thickness of mortar layer would also impact positively on the cost of the bahareque wall while maintaining a good behavior at non-linear stage. Also, it is shown how the increase of nails would increase the shear capacity at the lowest cost of the materials, reaffirming that an optimal configuration would be with a 15 mm mortar layer and an increased nailing reinforcement.

4 Conclusion

This study developed a numerical framework using OpenSees to represent the cyclic behavior and energy dissipation of cemented bahareque walls. The model was calibrated against past experimental tests to capture the non-linear response, stiffness degradation, and hysteretic behavior under reversed cyclic loading, providing a basis for analyzing and optimizing these walls as an affordable seismic-resistant housing solution. An additional sensitivity study was performed, enabling an evaluation of geometric, material, and loading variables to the lateral response. The main results are outlined below.

- The validated OpenSees model predicts the cyclic behavior of cemented bahareque walls with a relative energy error of 4.84%, and peak force errors of 1.3% (positive) and 0.8% (negative), confirming robust accuracy below 10% and realistic stiffness degradation and hysteresis.
- The sensitivity analysis confirms that fastener spacing most significantly affects strength capacity and energy dissipation, with an increase from 160 mm to 200 mm improving capacity by 23.4% through better load distribution and reduced fastener stress, which also enhances out-of-plane stability.
- Reducing fastener spacing to 120 mm decreases capacity by 22.87%, showing that excessive fastening can overstress

materials, while changes in aspect ratio from 1.00 to 1.25 reduce strength by 18.26% but maintain higher force at larger drifts, highlighting the trade-off between stability and lateral load capacity.

- Reducing the reinforcement quantity (mortar layer thickness) from 25 mm to 15 mm or the cross-section size of frame elements slightly enhances the behavior of the bahareque wall. Combining reduced mortar thickness with increased fastener diameter and spacing provides cost-effective solutions with improved lateral load capacity and efficient energy dissipation.

Data availability statement

The original contributions presented in the study are included in the article/supplementary material, further inquiries can be directed to the corresponding author.

Author contributions

NG-T: Software, Funding acquisition, Formal Analysis, Writing – original draft, Resources, Visualization, Supervision, Project administration, Validation, Investigation, Methodology, Conceptualization, Writing – review and editing, Data curation. JM-C: Writing – original draft, Visualization, Investigation, Software, Validation, Writing – review and editing, Formal Analysis. MV-P: Investigation, Formal Analysis, Writing – review and editing. HZ-M: Project administration, Writing – review and editing, Investigation, Funding acquisition. KT-A: Investigation, Writing – review and editing, Methodology, Validation. DB: Writing – review and editing, Methodology, Validation. DB: Writing – review and editing, Methodology, Validation. DB: Writing – original draft.

Funding

The author(s) declared that financial support was not received for this work and/or its publication.

Conflict of interest

The author(s) declared that this work was conducted in the absence of any commercial or financial relationships that could be construed as a potential conflict of interest.

Generative AI statement

The author(s) declared that generative AI was not used in the creation of this manuscript.

Any alternative text (alt text) provided alongside figures in this article has been generated by Frontiers with the support of artificial intelligence and reasonable efforts have been made to ensure accuracy, including review by the authors wherever possible. If you identify any issues, please contact us.

Publisher's note

All claims expressed in this article are solely those of the authors and do not necessarily represent those of their affiliated

organizations, or those of the publisher, the editors and the reviewers. Any product that may be evaluated in this article, or claim that may be made by its manufacturer, is not guaranteed or endorsed by the publisher.

References

- Abdul-Qadir, A., and Saeed, J. (2020). In-plane shear strengthening of masonry walls after damage. *Sulaimani J. Eng. Sci.* 7 (1), 65–85. doi:10.17656/sjes.10122
- Adheem, A. H., Kadhim, M. M. A., Jawdhari, A., and Altaee, M. J. (2022). *Application of drucker-prager plasticity model for concrete confined with Fiber Reinforced Cementitious Mortar (FRCM)*. Ghent, Belgium: European Alliance for Innovation (EAI). doi:10.4108/eai.7-9-2021.2315489
- Aranha, C., Branco, J., Lourenco, P., Flatscher, G., and Schickhofer, G. (2016). *Finite element modelling of the cyclic behaviour of CLT connectors and walls*. Vienna, Austria: Technische Universität Wien.
- Arbelaez, J., and Correal, J. F. (2012). Racking performance of traditional and non-traditional engineered bamboo shear walls. *Key Eng. Mater.* 517, 171–178. doi:10.4028/www.scientific.net/KEM.517.171
- ASTM International. (2019). *Standard test methods for cyclic (Reversed) load test for shear resistance of vertical elements of the lateral force resisting systems for buildings (issues E2126–19)*. West Conshohocken, PA: ASTM International. doi:10.1520/E2126-19
- Blondet, M., Torrevalva, D., Vargas, J., Tarque, N., and Velásquez, J. (2006). Seismic reinforcement of adobe houses. In: *Proceedings of 1st European conference on earthquake engineering and seismology*, Pavia, Italy: European Association for Earthquake Engineering (EAAE). 3–8.
- Cao, J., Xiong, H., Liu, Y., Yu, D., and Chen, J. (2022). Seismic performance of glulam timber post and beam structures with and without light frame timber wall infill. *J. Build. Eng.* 57, 104965. doi:10.1016/j.job.2022.104965
- Casagrande, D., Rossi, S., Sartori, T., and Tomasi, R. (2016). Proposal of an analytical procedure and a simplified numerical model for elastic response of single-storey timber shear-walls. *Constr. Build. Mater.* 102, 1101–1112. doi:10.1016/j.conbuildmat.2014.12.114
- Cristancho, K., Ruiz, D. M., Barrera, N., Villalba-morales, J. D., Alvarado, Y. A., and Cundum, O. (2025). *Seismic behavior of bahareque walls under In-Plane horizontal loads*, Basel, Switzerland: MDPI. 1–25.
- Di Gangi, G., Demartino, C., Quaranta, G., and Monti, G. (2020). Dissipation in sheathing-to-framing connections of light-frame timber shear walls under seismic loads. *Eng. Struct.* 208, 110246. doi:10.1016/j.engstruct.2020.110246
- Dong, H., He, M., Wang, X., Christopoulos, C., Li, Z., and Shu, Z. (2021). Development of a uniaxial hysteretic model for dowel-type timber joints in OpenSees. *Constr. Build. Mater.*, 288, 123112. doi:10.1016/j.conbuildmat.2021.123112
- Echeverry, J. S., Correal, J. F., and Orozco, A. F. (2017). *Incremental dynamic analysis of a five-story laminated guadua bamboo framed building 2877*. Santiago, Chile: Chilean Association of Seismology and Earthquake Engineering (ACHISINA).
- Farnam, S. M., and Khorshidi, M. (2023). Numerical analysis of J-Hook connectors' effect on the performance of steel-concrete composite shear walls. *J. Rehabilitation Civ. Eng.* 11 (2), 94–112. doi:10.22075/JRCE.2022.23015.1494
- Gattesco, N., and Boem, I. (2016). Stress distribution among sheathing-to-frame nails of timber shear walls related to different base connections: experimental tests and numerical modelling. *Constr. Build. Mater.* 122, 149–162. doi:10.1016/j.conbuildmat.2016.06.079
- González, G., and Gutiérrez, J. (2005). Structural performance of bamboo "bahareque" walls under cyclic load. *J. Bamboo Rattan* 4 (4), 353–368. doi:10.1163/156915905775008345
- González Beltrán, G. (2023). Experimental testing of wood framed walls with available materials in Costa Rica. *Ingeniería* 33 (2), 1–16. doi:10.15517/ri.v33i2.52390
- Guan, M., Hang, X., Wang, M., Zhao, H., Liang, Q. Q., and Wang, Y. (2024). Development and implementation of shear wall finite element in OpenSees. *Eng. Struct.* 304 (November 2023), 117639. doi:10.1016/j.engstruct.2024.117639
- Hao, J. P., Cai, Z. P., and Kou, Y. F. (2023). Effect of diagonal bamboo strips on seismic behavior of sprayed composite mortar-original bamboo composite walls: an experimental study. *J. Build. Eng.* 79 (September), 107829. doi:10.1016/j.job.2023.107829
- Hu, D., Li, G., Sun, F., and Wang, K. (2007). Seismic response analysis of semi-rigidly connected composite frames. *Earthq. Resist. Eng. Retrofit.* 1, 19–25. doi:10.16226/j.issn.1002-8412.2007.01.004
- Hutubessy, V. R. R., Priyosulistyo, H., and Awaludin, A. (2014). The material behavior of plastered-bamboo wall towards lateral loads. *Int. J. Eng. Res. Appl. (IJERA)* 4, 397–403. Available online at: https://www.ijera.com/papers/Vol4_issue1/Version%202/BD4102397403.pdf.
- Kaminski, S., Felipe López, L., Trujillo, D. J. A., and Escamilla, E. Z. (2023). Composite bamboo shear walls-A shear wall system for affordable and sustainable housing in tropical developing countries. In: *SECED 2023 - Earthquake Engineering Dynamics for a Sustainable Future*. doi:10.3929/ethz-b-000633112
- Lu, X., Xie, L., Guan, H., Huang, Y., and Lu, X. (2015). A shear wall element for nonlinear seismic analysis of super-tall buildings using OpenSees. *Finite Elem. Analysis Des.* 98, 14–25. doi:10.1016/j.fin.2015.01.006
- Lu, Y., Lv, Q., and Liu, Y. (2022). Experimental and numerical study on seismic performance of CLB rocking wall with bending-friction coupled dampers. *J. Build. Eng.* 45 (August 2021), 103622. doi:10.1016/j.job.2021.103622
- Lukic, R., Poletti, E., Rodrigues, H., and Vasconcelos, G. (2018). Numerical modelling of the cyclic behavior of timber-framed structures. *Eng. Struct.* 165 (March), 210–221. doi:10.1016/j.engstruct.2018.03.039
- Luna, P., and Takeuchi, C. (2012). Experimental analysis of frames made with glued laminated pressed bamboo guadua. *Key Eng. Mater.* 517, 184–188. doi:10.4028/www.scientific.net/KEM.517.184
- Mali, P. R., and Datta, D. (2018). Experimental evaluation of bamboo reinforced concrete slab panels. *Constr. Build. Mater.* 188, 1092–1100. doi:10.1016/j.conbuildmat.2018.08.162
- McKenna, F. (2011). OpenSees: a framework for earthquake engineering simulation. *Comput. Sci. Eng.* 13 (4), 58–66. doi:10.1109/MCSE.2011.66
- McKenna, F., Fenves, G. L., Scott, M. H., Stojadinović, B., and Jeremić, B. (2025). *OpenSees - Open system for earthquake engineering simulation*, Version 3.7.1.
- MIDUVI (2015). Norma Ecuatoriana de la Construcción: NEC-SE-GUADUA. In: *Ministerio de Desarrollo Urbano y Vivienda (MIDUVI)*. Quito, Ecuador: Ministerio de Desarrollo Urbano y Vivienda (MIDUVI). Available online at: <https://www.habitatvivienda.gob.ec/wp-content/uploads/downloads/2017/04/NEC-SE-GUADUA-VERSION-FINAL-WEB-MAR-2017.pdf>.
- Mite-Anastacio, F., Tello-Ayala, K., García-Troncoso, N., Silva, C. E., Malaga-Chuquitaype, C., Arévalo, K., et al. (2022). Structural behavior of cemented bahareque for social housing: a case study in Guayaquil City, Ecuador. *Front. Built Environ.* 8 (October), 1–20. doi:10.3389/fbuil.2022.922397
- Ogrizovic, J., Abbiati, G., Stojadinović, B., and Frangi, A. (2022). Hybrid simulation of a post-tensioned timber frame and validation of numerical models for seismic design. *Eng. Struct.* 265 (May), 114415. doi:10.1016/j.engstruct.2022.114415
- Oh, S., Kim, T., and Song, J. (2023). Bouc-wen class models considering hysteresis mechanism of RC columns in nonlinear dynamic analysis. *Int. J. Non-linear Mech.* 148, 104263. doi:10.1016/j.ijnonlinmec.2022.104263
- Parisse, F., Poletti, E., Dutu, A., and Rodrigues, H. (2021). Numerical modeling of the seismic performance of Romanian timber-framed masonry walls. *Eng. Struct.* 239 (March), 112272. doi:10.1016/j.engstruct.2021.112272
- Patton-Mallory, M., Gutkowski, R. M., and Soltis, L. A. (1984). Racking performance of light-frame walls sheathed on two sides. In: *USDA Forest Service Research Paper FPL* (Madison, WI: Forest Products Laboratory). Available online at: <https://www.fpl.fs.usda.gov/documnts/fplrp/fplrp448.pdf>.
- Poletti, E., Vasconcelos, G., Branco, J. M., and Koukouviki, A. M. (2016). Performance evaluation of traditional timber joints under cyclic loading and their influence on the seismic response of timber frame structures. *Constr. Build. Mater.* 127 (October), 321–334. doi:10.1016/j.conbuildmat.2016.09.122
- Puri, V., Chakraborty, P., Anand, S., and Majumdar, S. (2017). Bamboo reinforced prefabricated wall panels for low cost housing. *J. Build. Eng.* 9 (November 2016), 52–59. doi:10.1016/j.job.2016.11.010
- Quinn, N., Dayala, D., and Descamps, T. (2016). Structural characterization and numerical modeling of historic quincha walls. *Int. J. Archit. Herit.* 10 (2–3), 300–331. doi:10.1080/15583058.2015.1113337
- Resmi, R., and Yamini Roja, S. (2016). A review on performance of shear wall. *Int. J. Appl. Eng. Res.* 11 (3), 369–373. Available online at: https://www.researchgate.net/publication/301324383_A_REVIEW_ON_PERFORMANCE_OF_SHEAR_WALL.
- Shabani, A., and Ykioumarsi, M. (2022). A novel macroelement for seismic analysis of unreinforced masonry buildings based on MVLEM in OpenSees. *J. Build. Eng.* 49 (October 2021), 104019. doi:10.1016/j.job.2022.104019
- Shamim, I., and Rogers, C. A. (2013). Steel sheathed/CFS framed shear walls under dynamic loading: numerical modelling and calibration. *Thin-Walled Struct.* 71, 57–71. doi:10.1016/j.tws.2013.05.007

- Shan, B., Qiu, J., Xu, H., Li, T., Xiao, Y., Qin, S., et al. (2023). Experimental research on standardized bamboo culm components for developing prefabricated bamboo building. *Structures* 50 (February), 272–285. doi:10.1016/j.istruc.2023.02.046
- Sharma, B., Mitch, D., Harries, K. A., Ghavami, K., and Kharel, G. (2011). Pushover behaviour of bamboo portal frame structure. *Int. Wood Prod. J. 2* (1), 20–29. doi:10.1179/2042645311Y.0000000003
- Sharma, B., Gatóo, A., and Ramage, M. H. (2015). Effect of processing methods on the mechanical properties of engineered bamboo. *Constr. Build. Mater.* 83, 95–101. doi:10.1016/j.conbuildmat.2015.02.048
- Vieux-Champagne, F., Sieffert, Y., Grange, S., Polastri, A., Ceccotti, A., and Daudeville, L. (2014). Experimental analysis of seismic resistance of timber-framed structures with stones and earth infill. *Eng. Struct.* 69, 102–115. doi:10.1016/j.engstruct.2014.02.020
- Wang, R., Wei, S. Q., Li, Z., and Xiao, Y. (2019). Performance of connection system used in lightweight glulam shear wall. *Constr. Build. Mater.* 206, 419–431. doi:10.1016/j.conbuildmat.2019.02.081
- Yan, J. B., Richard Liew, J. Y., and Zhang, M. H. (2015). Shear-tension interaction strength of j-hook connectors in steel-concrete-steel sandwich structure. *Adv. Steel Constr.* 11 (1), 73–94. doi:10.18057/ijasc.2015.11.1.5
- Yan, X., Shi, S., Wang, F., and Mao, H. (2024). Seismic fragility analysis of prefabricated self-centering frame structure. *J. Constr. Steel Res.* 220 (June), 108843. doi:10.1016/j.jcsr.2024.108843
- Yang, G., and Wang, K. (2020). Evaluation on the application of GLB structures. *J. Mater. Sci. Chem. Eng.* 08 (05), 21–37. doi:10.4236/msce.2020.85003
- Yang, L., Zheng, S.-S., Zheng, Y., Dong, L.-G., and Wu, H.-L. (2023). Experimental investigation and numerical modelling of the seismic performance of corroded T-shaped reinforced concrete shear walls. *Eng. Struct.*, 283, 115930. doi:10.1016/j.engstruct.2023.115930
- Yu, S., Zhang, Y., Bie, J., Zhang, W., Jiang, J., Chen, H., et al. (2023). Finite element analysis of hysteretic behavior of superposed shear walls based on OpenSEES. *Buildings* 13 (6), 1382. doi:10.3390/buildings13061382
- Zambrano, H., García, N., Molina, J., Tello, K., Vergara, M., Sosa, D., et al. (2025). Experimental assessment of the lateral cyclic response of cemented bahareque walls. *Results Eng.*
- Zhao, J. C., and Qiu, H. X. (2023). Seismic performance assessment of a multi-story bamboo frame structure. *Adv. Bamboo Sci.* 2 (August 2022), 100011. doi:10.1016/j.bamboo.2022.100011